Steric and Substrate Mediation of Polymers Formed within Single Molecular Layers

Mark D. Mowery and Christine E. Evans*

Department of Chemistry, University of Michigan, 930 N. University Ave., Ann Arbor, Michigan 48109-1055

Received: April 8, 1997; In Final Form: July 29, 1997[⊗]

The fabrication of well-defined interfacial structures has been recently facilitated by incorporating diacetylenic structures within spontaneously formed monolayer assemblies. Photoinduced polymerization within these single molecular layers provides a robust system for interfacial design that can be controlled using phototemplating. In this paper, we examine the control of molecular structure within this single molecular layer by introducing internal and external perturbations to the monolayer fabrication process. Internal steric perturbations are assessed by incorporation of an ester moiety below the polymer backbone. Direct comparison of monolayer structures formed using analogous precursors with and without the ester functionality indicates significant disruption in the alkyl crystallinity in the region below the polymer backbone. Despite the considerable constraints on the structural order required for successful polymerization, this steric disruption does not appear to significantly limit the polymerization process. The effect of external perturbations on monolayer polymerization is evaluated using an atomically rough substrate. Under these conditions, selective polymerization appears to occur in the interstitial regions between substrate features. Such localized polymerization has clear implications for nanoscale templating in the fabrication of well-defined interfacial structures. Further control over the interfacial chemistry is facilitated by the addition of a secondary adsorbate after monolayer polymerization. This combination of internal and external control over monolayer fabrication makes possible both the long- and short-range control of interfacial chemistry that is important for applications ranging from sensor design to adhesion studies.

Introduction

Alkanethiols and disulfides are widely known to spontaneously assemble into monolayer films on gold (111) surfaces in a $\sqrt{3} \times \sqrt{3}$ *R*30° overlayer structure tilted 30−40° from the surface normal.[1−3] The monolayers are stabilized by a 44 kcal/mol adsorption energy and the van der Waals interactions between alkyl chains within the monolayer.[1−4] The contribution of the van der Waals interactions to the overall stability of these monolayers becomes more significant with increasing chain length, leading to an increase in structural order and electron-transfer inhibition properties with chain length.[4] However, even with the enhanced stabilization, the applicability of conventional long-chain alkanethiol and disulfide monolayers is often limited by durability. This limitation has been recently overcome using spontaneous assembly and subsequent topochemical photopolymerization of alkanethiol or disulfide compounds containing conjugated diacetylene groups (Figure 1A).[5−7] The incorporation of the polymer backbone within the monolayer structure leads to significant improvement in the overall film stability and robustness under a wide range of solvent conditions.[8,9] Direct covalent linkage between individual adsorbates generates considerable stability in addition to that already present from the van der Waals interactions and gold−sulfur bonds, improving the durability of the polymerized structures. Many of the physical and chemical properties of these polymerized monolayers are not widely attainable in conventional monolayer systems and are attractive for applications ranging from lubrication/adhesion to photoelectronics and sensor design. The conjugated polymer backbone inherent in these monolayers provides unique optical and electronic properties that are sensitive to the local structural environment of the monolayer. Furthermore, the polymerization process within these monolayers is regulated by strict intermolecular spatial requirements between conjugated triple bonds in the monomer species (Figure 1B).[10,11] This structural dependence of polymerization suggests that factors, both internal and external to the monolayer structure that affect the spatial orientation of the monomers, may significantly alter the polymerization process and the overall properties of the resultant monolayer.

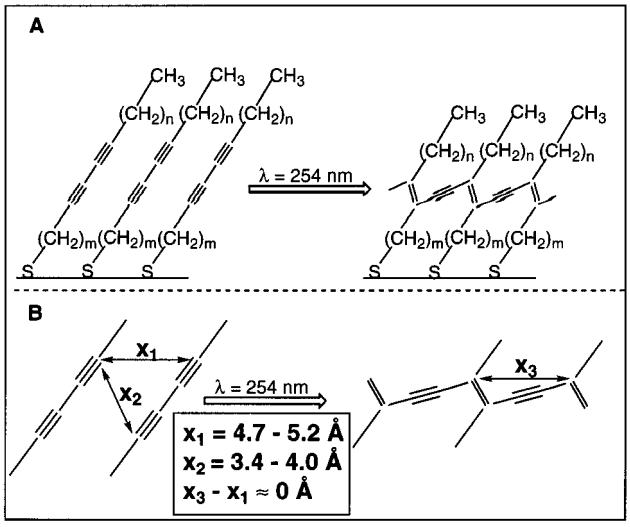

Figure 1. (A) Diagram of polymerization of self-assembled monolayers containing conjugated diacetylene groups. (B) Intermolecular spatial constraints for polymerization.

Polydiacetylenes, first reported by Wegner,[12] have been extensively studied as crystals, thin and thick films, and Langmuir−Blodgett assemblies.[13] Of interest for their unique optical and electronic properties, polydiacetylenic compounds have been investigated for applications including nonlinear optical materials, photoresists, and chemical sensors.[14−18] However, the utilization of polydiacetylenes in spontaneously

* Corresponding author. Fax 313-647-4865; e-mail CEEVANS@UMICH.EDU.

[⊗] Abstract published in *Advance ACS Abstracts,* September 15, 1997.

S1089-5647(97)01209-1 CCC: $14.00

assembled monolayer systems was only recently demonstrated by Batchelder et al. for the preparation of methyl-terminated polymerized diacetylene monolayers on gold surfaces.[6] Studies by Crooks et al. have since extended this research to include hydroxyl- and carboxy-terminated diacetylene thiols.[7,8,18,19] These reports confirm the feasibility of two-dimensional photopolymerization of conjugated diacetylene compounds on gold surfaces, as well as predictions that the durability to solvent, electrochemical, and temperature extremes is dramatically improved by the incorporation of the conjugated polymer backbone into alkanethiol or disulfide monolayers.

Polymerization in compounds containing conjugated diacetylene groups is critically dependent on the intermolecular separation (Figure 1B), with tolerances on both lateral and vertical displacement between alkyne groups on neighboring molecules of approximately 0.5 Å.[10,11] As a result of this spatial dependence, satisfactory polymerization requires significant local structural order in regions near the sites of unsaturation. For applications to spontaneously assembled systems, the equilibrium binding sites of the sulfur headgroups on a gold surface fortuitously positions the diacetylene groups within the spatial constraints necessary for polymerization. Furthermore, alterations in the structure of the alkyl side chains upon polymerization are not expected because significant lateral constriction of the monolayer structure does not occur upon polymerization ($x_3 - x_1$ in Figure 1B).[10,11] While the constraint on lateral polymerization is satisfied by the spatial distribution of the sulfur binding sites, the vertical constraint may be locally exceeded at atomic step sites on the gold surface. This possibility may require significant control over the gold substrate surface roughness before wide ranging control over the structural properties of these polymerized monolayers can be realized.

In this paper, we demonstrate that parameters affecting the relative spatial orientation of diacetylene monomer species adsorbed to a gold surface may significantly alter the overall structure and properties of the polymerized monolayer. We have synthesized the following structurally analogous precursors for direct comparison of internal steric constraints on monolayer structure,

$$[CH_3(CH_2)_nC{\equiv}C-C{\equiv}C(CH_2)_mS-]_2 \quad \text{(I)}$$

$$[CH_3(CH_2)_nC{\equiv}C-C{\equiv}C(CH_2)_mOOC(CH_2)_2S-]_2 \quad \text{(II)}$$

with $m = 9$ and $n = 7$, 11, and 15. The designation 15,9-PDA is utilized to indicate a polymeric structure with $n = 15$ and $m = 9$, and alkyl and ester identification is used to specify monolayers formed using structures I and II, respectively. By varying the length above the polymer backbone (n) while maintaining a constant length from the backbone to the surface (m), the affects of both chain length and steric limitations imposed by the ester linkage on the polymerized monolayer structure are evaluated. Finally, locally confined polymerization is examined by using the substrate topography to impose external spatial limitations on the monolayer structure. Ultimately, the feasibility of controlling the physical and chemical properties of the interfacial structure on a nanoscopic scale is explored for future applications in interfacial design.

Experimental Methods

Monolayer Fabrication. The synthesis of the straight alkyl chain diacetylene disulfides followed the method recently reported by our laboratory.[5] Preparation of the diacetylene disulfides containing an ester functional group utilized the synthetic method described by Batchelder et al.[6] Gold substrates were prepared by sputtering 200 nm gold (≥99.99%) onto freshly cleaved green mica (ASTM V-2; Asheville-Schoonmaker Mica Co.) using an electrical discharge deposition system (Denton Desk II). Upon sputtering, the gold films were immediately immersed in a 1 mM chloroform solution of the disulfide or thiol of interest and allowed to equilibrate at room temperature for 18−24 h. Strict light control was maintained during the preparation and storage of the diacetylene solutions and monolayer films. The substrates were then removed and rinsed extensively with chloroform (Aldrich, > 99%) and deionized water (Model UV Plus Milli-Q, Millipore, >18 MΩ) and dried under nitrogen. The resulting diacetylene monolayers were subsequently polymerized with a low-intensity UV lamp (Model UVG-11, Ultra-Violet Products Inc.) at a distance of 1 cm (254 nm, power density ∼0.05 W/cm^2). After polymerization, these monolayer polymer films were rinsed again with chloroform and water, followed by drying under nitrogen.

Raman Spectroscopy. Spectra were obtained using an imaging system consisting of a microscope (BH-2, Olympus) objective (20X, 0.46 NA), a 50/50 beam splitter, a spectrograph (Holospec f/1.8i VPT; Kaiser), and a CCD camera (Photometrics). The 632.8 nm line of a He−Ne laser (35 mW) was utilized for excitation.

Fourier-Transform Infrared Spectroscopy. Grazing-angle FTIR experiments were accomplished using a nitrogen-purged Nicolet 550 Magna IR spectrometer with a liquid nitrogen-cooled MCT detector. Spectra were obtained with a Spectra-Tech Inc. specular reflectance accessory using p-polarized light incident on the samples at 85° with respect to normal. All spectra were taken as the average of 1024 scans with a resolution of 2 cm^{-1} and were referenced against an unmodified gold film.

Electrochemistry. All of the electrochemistry experiments were performed with a Bioanalytical systems CV-27 potentiostat and a Hewlett-Packard 7035B X−Y recorder. The cyclic voltammetry experiments utilized a standard three-electrode cell with a double-junction Ag/AgCl reference electrode (saturated KCl internal solution) and a coiled platinum wire counter electrode. The area of the working electrode was 0.95 cm^2, as defined by an inert elastomer O-ring, and all solutions were prepared immediately before use with ultrahigh-purity water. Interfacial capacitances were determined at 0.0 V by cyclic voltammetry at 100 mV/s in 0.5 M KCl.

Atomic Force Microscopy. AFM imaging measurements utilized a Digital Instruments Inc. Nanoscope III multimode scanning probe microscope operated in ambient conditions. Images were acquired in the tapping mode using silicon cantilevers with integral tips. The spring constants of the tips were not directly determined but were estimated by the manufacturer to be between 20 and 100 N/m. Images were obtained by oscillating the cantilever slightly below its resonance frequency (typically 200−300 kHz) and raster scanning across the surface while tapping the tip against the substrate.

Results and Discussion

Topochemical polymerization in diacetylenes is known to be highly dependent on the proximity and the relative orientation of monomers (Figure 1B). When considering single molecular layers, both the monomer interaction distance and the substrate surface structure may significantly affect polymerization. In this paper, we examine the role of internal steric restrictions by direct comparison of straight alkyl chain diacetylene monomers (I) with their analogues incorporating an ester linkage near the surface (II). The impact of substrate-induced variations in height is evaluated using gold surfaces with significant deviations in surface topography. While these factors may complicate the

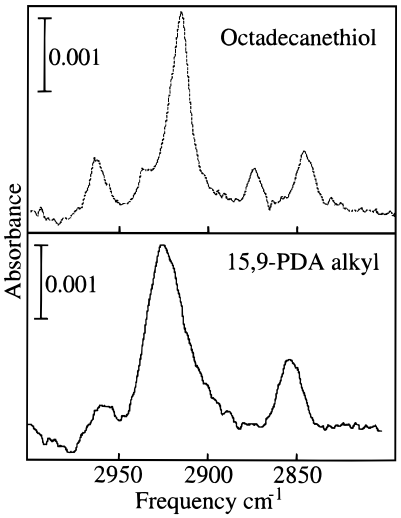

Figure 2. FTIR spectra collected at a grazing angle of 85° and a resolution of 2 cm^{-1}.

polymerization process, careful manipulation of these perturbation parameters provides a means for the nanoscale control of interfacial design.

Spectroscopic Characterization. Preliminary characterization of monolayer polymerization is accomplished using Raman spectroscopy. The alkene stretch, completely absent in the unpolymerized monolayer, is prominent in the polymerized layer. The measured frequency for both the alkene and alkyne stretching vibrations (1469 and 2088 cm^{-1}, respectively) are considerably lower than those expected for isolated vibrations (1620 and 2260 cm^{-1}, respectively). This decrease is consistent with the expected electronic delocalization within the polymer backbone region.[20] Although quantitation of the extent of polymerization is difficult due to possible resonance enhancement, the prominent presence of the alkene stretch and the decrease in vibrational frequencies indicates a significant degree of polymerization within the monolayer structure.

Molecular-scale order within the alkyl region of the polymerized monolayer is evaluated using Fourier-transform infrared spectroscopy at a grazing angle (85° with respect to normal). Highly sensitive to the average molecular-scale structure, the C−H stretching vibrations within highly crystalline alkyl chains are approximately 2918 cm^{-1} for the asymmetric and 2851 cm^{-1} for the symmetric stretching frequencies.[4] With increasing disorder and a less constricted environment, vibrational frequencies are expected to systematically increase. Thus, a high-density monolayer with alkyl chains in the all-trans conformation is predicted to have C−H asymmetric and symmetric stretches near those of highly ordered crystalline-like phases, and a less densely packed monolayer with many cis defect sites should have C−H asymmetric and symmetric stretches shifted to higher energy. Representative spectra of an octadecanethiol monolayer and a 15,9-PDA alkyl monolayer are illustrated in Figure 2. Because the spectra of all other PDA monolayers vary only in position and magnitude, frequency measurements for the polymerized monolayers are summarized in Table 1 with octadecanethiol monolayer measurements listed for comparison. Both the alkyl- and ester-containing polymerized layers show C−H stretching frequencies that are shifted to a greater frequency relative to the highly ordered octadecanethiol monolayer. Although the constraints for polymerization require considerable molecular order (Figure 1B), the C−H stretching frequencies of the polymerized monolayers suggest a significant degree of disorder within the alkyl chain structure. This lack of crystalline behavior is also in contrast with Raman measurements that show the presence of CH_2 rocking and wagging modes between 1300 and 1400 cm^{-1}, indicating a significant degree of order associated with the alkyl chains. Thus, the polymerized layer appears to consist of regions with a high degree of local order together with regions that are more disordered. This distribution of ordered states may be further assessed using the full width at half-maximum (fwhm) of the C−H stretching transitions. A narrow distribution of frequencies is indicative of a uniformly ordered structure, whereas a broader distribution indicates heterogeneity in the structural order. For the systems of interest here, a significant increase in the fwhm of the polymerized monolayers is observed relative to octadecanethiol (Table 1). This result is fully consistent with the supposition that a single layer of PDA exhibits a distribution of local environments. This variation in local order within the alkyl chains may be caused by decreased packing density originating from steric limitations imposed by the conjugated triple bonds in the monomer.[21] That is, the unsaturated monomer structure effectively acts as cis defect sites, leading to a less crystalline packing of the alkyl chains. For all monolayers shown here, no significant change in C−H stretching vibrations occurs upon polymerization, indicating that any disruption in order caused by the conjugated triple bonds is retained in the polymerized structure. This lack of perturbation upon polymerization is not unexpected since no significant lateral expansion or contraction upon polymerization is observed in crystal structure studies. Finally, the combination of the strict spatial requirements for polymerization and the surface roughness may cause incomplete polymerization, and the resulting spatial defect sites would also lead to less ordered regions at grain boundaries. Studies are presently underway to distinguish these contributions to the overall distribution of order within the monolayer structure.

TABLE 1: Infrared Spectroscopic Peak Positions of C−H Stretching Modes for Self-Assembled Monolayers on Sputtered Gold/Mica[a]

monolayer	ν_a(C−H)	fwhm	ν_s(C−H)	fwhm
1-octadecanethiol	2918	12	2850	9
15,9-PDA ester	2927	20	2853	14
11,9-PDA ester	2927	24	2853	15
7,9-PDA ester	2930	31	2856	18
15,9-PDA alkyl	2922	24	2853	14
11,9-PDA alkyl	2925	22	2853	17
7,9-PDA alkyl	2928	26	2855	18

[a] All values are reported in cm^{-1} with an error in replicate determinations of ± 1 cm^{-1}.

Internal steric limitations to polymerization may be evaluated by direct comparison of spectroscopic characteristics for analogous monolayer films containing either straight alkyl chains or ester linkages near the surface. Consistent with observations for *n*-alkanethiol monolayers, the frequency of the C−H asymmetric stretch in these polymerized systems generally decreases with increasing chain length. However, a systematic increase in frequency is exhibited for the ester-containing monolayers relative to their complementary straight alkyl chain analogues, indicating disorder induced by the presence of the ester moiety. In addition to differences in the absolute frequency, the ester-containing analogues also display a general increase in fwhm for the C−H asymmetric stretch relative to their alkyl counterparts. Based on these results, the ester moiety not only perturbs the average crystallinity of the alkyl chains but also acts to increase the distribution of crystalline states. Thus, internal steric limitations imposed by chemical functionality can create significant variations in the local order within these polymerized monolayers. It should be noted that the ester-containing diacetylene monomers have an increased length in

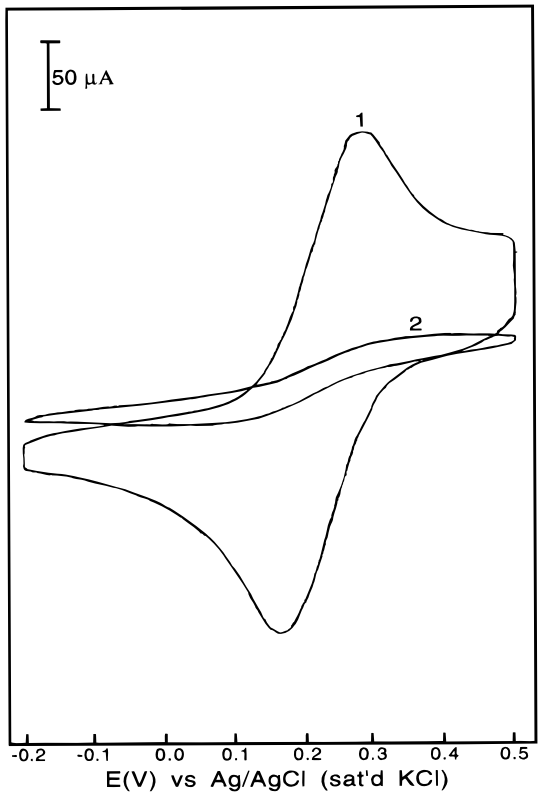

Figure 3. Cyclic voltammetric current response vs applied potential for (1) bare sputtered gold/mica and (2) 1-octadecanethiol on sputtered gold/mica. The solution is 1.0 mM in $Fe(CN)_6^-$ and 0.5 M in KCl. The sweep rate is 100 mV/s, and the temperature is 22 ± 1 °C.

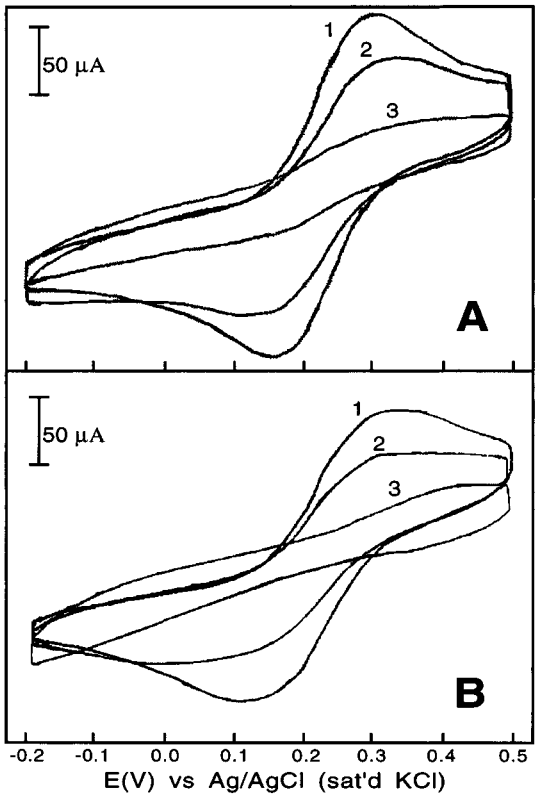

Figure 4. Cyclic voltammetric current response vs applied potential for (A) PDA with ester group and (B) PDA with alkyl chain. (1) 7,9-PDA, (2) 11,9-PDA, and (3) 15,9-PDA. Experimental conditions are identical with Figure 3, and nomenclature is as given in the text.

the region below the alkyne groups compared to their straight-chain counterparts. However, any order created by increased chain length is insufficient to overcome the steric disorder induced by the ester moiety. Ultimately, these spectroscopic studies demonstrate that a wide range of structural environments are accessible within single polymerized layers by variation of both chain length and internal functionality.

Electrochemical Characterization. Evaluation of the long-range structure of these polymerized monolayers is accomplished by heterogeneous electron-transfer experiments. Highly sensitive to spatial defects and overall film permeability, these electrochemical measurements offer insight into the inhibitory nature of the monolayer film to electron-transfer processes. For example, a monolayer completely covering the gold surface is expected to have no spatial defects where probe molecule penetration and electron transfer with the underlying metal can occur. In this ideal case, the closest approach of the redox probes will be defined by the thickness of the monolayer, and tunneling currents through the monolayer structure may be evident by a cyclic voltammogram displaying an exponential current increase.[4] Gold surfaces with monolayers containing a low density of nanometer to micron size spatial defects are expected to behave as an array of individual ultramicroelectrodes.[22,23] In the limiting case when the diffusion layers of each defect are independent, radial diffusion dominates the transport of probe molecules, and the voltammetric curve appears plateau-shaped at potentials beyond $E°$. Finally, for surfaces modified by monolayers exhibiting high defect densities that no longer behave independently, molecular transport occurs by linear diffusion to the metal surface, resulting in a peak-shaped cyclic voltammogram.[22,23]

The response of ferricyanide ion to potential cycling at a bare gold surface and a gold surface modified with an octadecanethiol monolayer is shown in Figure 3. The unmodified gold electrode exhibits classical behavior consistent with uninhibited diffusion. In contrast, the octadecanethiol-modified surface demonstrates a plateau-shaped cyclic voltammogram indicative of primarily radial diffusion to small defect sites, consistent with previous studies on sputtered gold surfaces.[24] Comparison with electron transfer at gold electrodes modified with polymerized monolayers (Figure 4) reveals significantly inhibited electron transfer; however, blocking characteristics are generally diminished relative to the octadecanethiol monolayer. These trends indicate an increase in number and/or size of spatial defects compared to octadecanethiol monolayers and are consistent with the variations in local order within the polymerized monolayers. Cyclic voltammetric measurements at electrodes modified with polymerized monolayers (Figure 4) also indicate that electron transfer is highly dependent on chain length, as observed for *n*-alkanethiol monolayers.[4] In this case, the peak-shaped current response curves of electrodes with 7,9-polymerized diacetylene monolayers show linear diffusion to many large spatial defects. As the number of methylene groups above the polymer backbone increases from 11 to 15, radial diffusion to the gold surface begins to dominate probe transport, and a gradual transformation from a peak-shaped response to the appearance of a plateau is observed. This trend toward radial diffusion with increasing chain length may be directly attributed to a diminution in size and/or number of defect sites and improved electron-transfer inhibition.

Internal steric limitations within the monolayer structure are also observed to have a significant effect on the electron-transfer properties of surfaces modified with these polymerized monolayers (Figure 4). This perturbation in electron transfer is apparent upon comparison of the voltammetric response of electrodes modified with analogous alkyl- and ester-containing polymer monolayers. The incorporation of the ester functionality into the resultant structure yields a clear decrease in blocking

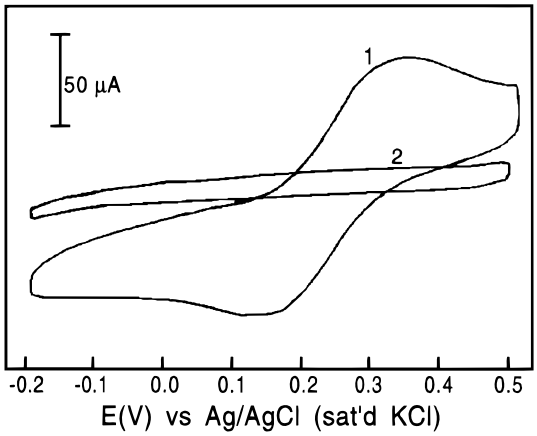

Figure 5. Cyclic voltammetric current response vs applied potential for (1) 11,9-PDA ester monolayer and (2) 11,9-PDA ester monolayer placed in a 1-octadecanethiol solution for 24 h. Experimental conditions are identical with Figure 3.

capability for the 7,9- and 11,9-PDA monolayers. Based on these data, an increase in the number and/or size of spatial defects is evident upon incorporation of the sterically limiting ester group into the monolayer structure. Together with spectroscopic evidence of disorder below the polymer backbone induced by the ester moiety, this increase in spatial defects infers a disruption in the packing structure of the resultant monolayer. The same decrease in blocking capability for the 15,9-PDA monolayers is not clearly observed. It is likely that the effect of added thickness on the faradaic current dominates the effect of the ester moiety. Studies are presently underway to quantitatively evaluate the impact of this steric disruption on the polymerization process.

Further control of the overall permeability of these polymerized structures is desirable for a broad range of applications including corrosion and sensor design. Feasibility of this control is demonstrated by the inhibition of electron transfer both before and after exposure to an octadecanethiol solution (Figure 5). The voltammetric response after immersion in the octadecanethiol solution reveals that the monolayer blocking characteristics improve dramatically. The increased inhibition to electron transfer is attributed to backfilling of spatial defects in the structure of the polymerized monolayer by octadecanethiol molecules. However, no perturbation in the frequency or fwhm of the C−H asymmetric stretch is observed upon incorporation of the secondary adsorbate. This result suggests that the crystallinity of the alkyl chains is not significantly altered upon backfilling and that these secondary adsorbate regions do not comprise a significant fraction of the monolayer structure. These observations are fully consistent with the previous assumption that probe molecule transport at surfaces modified by single-component polymerized monolayers occurs primarily by diffusion at defect sites and not permeation of the monolayer structure. Furthermore, capacitance measurements of the backfilled (42 μF/cm^2) compared to an octadecanethiol-modified surface (15 μF/cm^2) imply that the backfilled monolayer remains highly permeable to small ionic species in solution. Although this enhanced permeability may arise at small pinholes or defect boundaries, studies are currently underway to evaluate the small ion transport through the polymerized monolayer structure itself. Indeed, these polymerized layers appear to provide a means for the fabrication of single molecular layer structures with control over the permeability to a wide range of ion sizes.

Atomic Force Microscopy. Direct imaging of the topography of these spontaneously assembled polydiacetylene monolayers is accessible by atomic force microscopy.[25,26] Non-

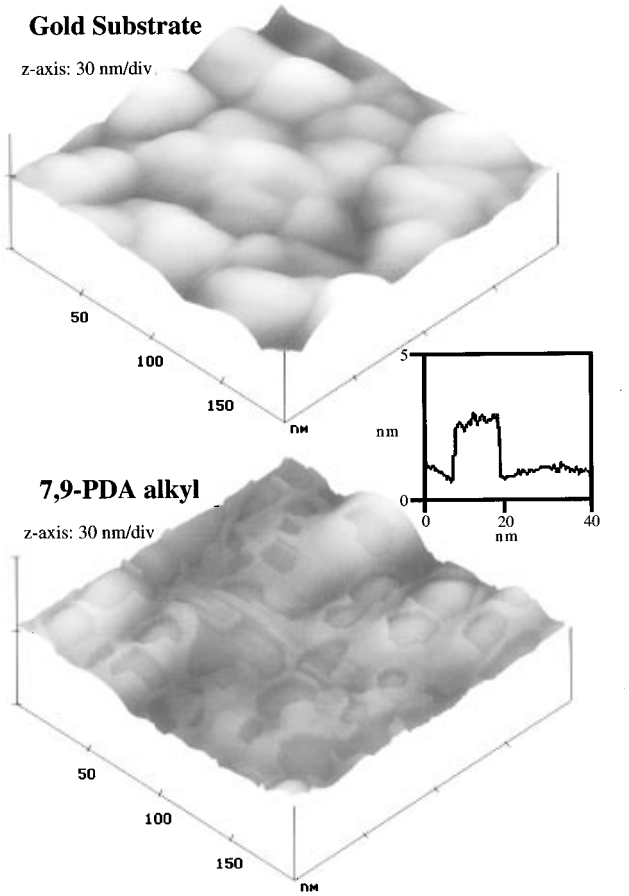

Figure 6. Atomic force microscope images collected in tapping mode with a silicon tip. The top image is the substrate of 200 nm sputtered gold on mica. The bottom image is the 7,9-PDA alkyl monolayer on 200 nm sputtered gold on mica, with the inset showing the height of the polymerized portion. Experimental details are as described in the text.

destructive imaging is facilitated by the conjugated polymer backbone which provides enhanced structural rigidity compared to monolayers fabricated with conventional alkanethiol or disulfide molecules. This rigidity enhances tapping-mode AFM as a viable alternative to conventional contact mode for imaging of these monolayer systems, based on the dependence of the cantilever deflection on polymer viscoelastic properties.[27]

The atomically rough gold substrates utilized in these studies make possible the evaluation of the role of substrate topography on the resultant monolayer film. The top image in Figure 6 shows a representative unmodified surface fabricated by sputtering gold onto freshly cleaved mica. Microscopically, these films exhibit features with dimensions of 1−10 nm in height by 10−50 nm in width and are characterized by a mean grain size of approximately 400 nm^2 (10 nm peak−peak). The lower image in Figure 6 shows the 7,9-alkyl chain polydiacetylene monolayer fabricated on these atomically rough surfaces. At first glance, this image appears to reveal less surface coverage than expected based on electron-transfer experiments. However, the AFM conditions chosen for these measurements are not expected to yield an image of the entire monolayer structure, but highlight those regions with a higher density of polymeric material. The tip spring constants of between 20 and 100 N/m utilized for these images are much greater than typically utilized for imaging simple alkyl-based monolayer structures. In fact, previous studies suggest that highly deformable structures would not be imaged under these conditions.[28] In this case, the AFM response is sensitive to the changes in mechanical properties of the monolayer upon polymerization, with regions containing

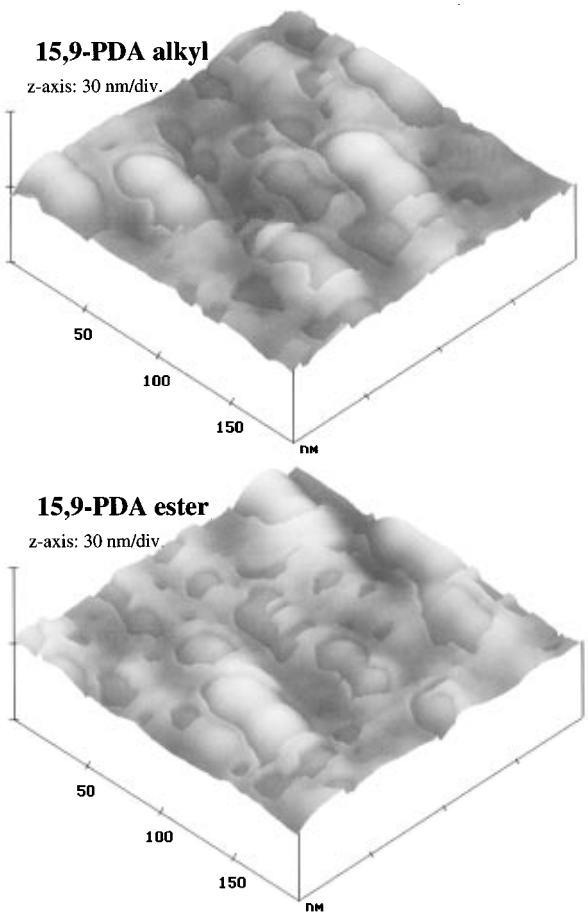

Figure 7. Atomic force microscope images collected under conditions identical with Figure 6. The top image is a 15,9-PDA alkyl monolayer, and the bottom image is a 15,9-PDA ester monolayer. Experimental details are as described in the text.

a high density of the polymerized portion exhibiting an increase in stiffness toward the silicon tip. As a result, the AFM response is expected to be greatly diminished in those regions of the monolayer that are unpolymerized, contain low local concentrations of polymer, or are comprised of small oligomers. Thus, the images obtained under these conditions appear to clearly reveal those regions of the monolayer structure that contain a higher concentration of polymerized molecules. The representative image shown in Figure 6 indicates that extensive polymerization is generally confined to the interstitial regions of the gold surface, with a limited quantity traversing the features. The cross section of the polymerized monolayer displayed in the inset to Figure 6 indicates a height of 1.9 nm. This value is consistent with the probability of deformation of the alkyl chains above the polymer backbone by the silicon tip. Indeed, the measured height is in general agreement with the distance of 1.5 nm expected from the surface to just above the polymer backbone, presuming an orientation of 20°.[2,19]

Comparison of images for the 11,9-PDA alkyl (not shown) and 15,9-PDA alkyl (Figure 7, top) indicates similar behavior to the 7,9-PDA alkyl monolayer. The highest density of polymerized material appears to reside in the interstitial regions, regardless of the chain length above the polymer backbone. Moreover, height measurements for these analogous monolayers reveal statistically identical values of 2.0 ± 0.2, 2.0 ± 0.4, and 2.1 ± 0.4 nm for the 7,9-PDA, 11,9-PDA, and 15,9-PDA, respectively. These observed height measurements are consistent with the hypothesis that the AFM image is sensitive to the structural rigidity of the polymer backbone. As a result, the alkyl region above the polymer backbone is not expected to significantly affect the measured height. This trend extends to precursors that incorporate the ester moiety (Figure 7, bottom). The presence of the ester does not appear to significantly alter the polymerization as indicated by the extent of coverage using AFM. Likewise, polymerization is primarily within the interstitial regions of these atomically rough gold substrates.

As clearly shown in Figures 6 and 7, the surface topography appears to play a significant role in polymerization within a single molecular layer. Since polymerization in diacetylenes is highly dependent on the intermolecular spacing between monomers, variations in surface topography may act to disrupt the polymerization process. Moreover, the regions between features may provide a spatially constrained environment to enhance the polymerization efficiency. Along with these spatial constraints, other possible origins for this localized polymerization include an enhanced electric field effect in the valley regions of the surface analogous to that observed in Raman spectroscopy, improved monomer orientation in the interstitial regions through local restructuring of the gold surface, and directed polymerization along terrace sites. Studies are presently underway to assess the affect of surface roughness and the potential origins of these substrate perturbations to monolayer polymerization.

The potential for light-induced perturbation affecting the resulting monolayer structure cannot be overlooked. In recent studies, photooxidation of the sulfur headgroups to sulfonates by ultraviolet radiation has been implicated as a mechanism for decreased structural integrity in spontaneously assembled thiol or disulfide monolayers on gold surfaces.[29−31] As a consequence, light-exposure conditions utilized in these studies were chosen to minimize the possibility of competition between photopolymerization and photooxidation. The absence of significant oxidation is evaluated, in part, by monitoring an octadecanethiol monolayer exposed to the same polymerization conditions as the polydiacetylene monolayers. In this case, electron-transfer experiments show no evidence of photoinduced defect sites, and spectroscopic measurements indicate no perturbation in structural order upon irradiation. In addition, no detectable alteration in the structural integrity of the polymerized monolayers is observed with an increased irradiation time of 10 min. Finally, direct comparison of films polymerized under nitrogen and air atmospheres exhibit no differences, eliminating photooxidation as a mechanism in the fabrication of these monolayer polymers.

Conclusions

Both internal steric and external substrate constraints are demonstrated to provide a significant degree of control in the fabrication of polydiacetylenic monolayers. Steric constraints caused by variations in monomer chain length and the incorporation of ester moieties are utilized to induce significant perturbations in the local order within the monolayer structure. These constraints are also shown to have a significant impact on the long-range structural order of these single-layer polymers. Using electron-transfer measurements, a clear trend from the linear to the radial diffusion domain is observed with increasing chain length which is characteristic of a diminution in size and/or number of spatial defect sites within the monolayer structure. In contrast, neither the chain length nor the presence of the ester functionality appears to significantly alter the polymerization properties as measured by AFM. On an atomically rough gold substrate, AFM imaging of these monolayer structures indicates that polymerization occurs selectively within the interstitial regions between features for all precursors. These results

suggest that polymerization within single molecular layers may be mediated by substrate topography. This working hypothesis regarding the role of surface roughness on monolayer polymers is currently under investigation. Moreover, studies are presently underway to utilize this nanoscale control over the interfacial structure to design and fabricate monolayer polymers on the nanometer to micrometer scale. Such capability makes polydiacetylene monolayers good candidates for surface patterning by locally controlling polymerization through a combination of light templating and variations in substrate topography.

Acknowledgment. The authors acknowledge the assistance of Prof. Michael Morris' group at the University of Michigan for their aid with Raman measurements. Acknowledgment is also made to the donors of the Petroleum Research Fund, administered by the American Chemical Society (#28332-G7), for partial support of this research. Additional support has been provided by the National Institute of General Medical Sciences, National Institutes of Health (#GM52555-01 A1).

References and Notes

(1) Ulman, A. *An Introduction to Ultrathin Organic Films*; Academic Press: New York, 1991 and references therein.

(2) Bain, C. H.; Troughton, E. B.; Tao, Y. T.; Evall, J.; Whitesides, G. M.; Nuzzo, R. G. *J. Am. Chem. Soc.* **1989**, *111*, 321.

(3) Dubois, L. H.; Nuzzo, R. G. *Annu. Rev. Phys. Chem.* **1992**, *43*, 437 and references therein.

(4) Porter, M. D.; Bright, T. B.; Allara, D. L.; Chidsey, C. E. D. *J. Am. Chem. Soc.* **1987,** *109*, 3559.

(5) Mowery, M. D.; Evans, C. E. *Tetrahedron Lett.* **1997**, *38*, 11.

(6) Batchelder, D. N.; Evans, S. D.; Freeman, T. L.; Haussling, L.; Ringsdorf, H.; Wolf, H. *J. Am. Chem. Soc.* **1994**, *116*, 1050.

(7) Kim, T.; Crooks, R. M. *Tetrahedron Lett.* **1994**, *35*, 9501.

(8) Kim, T.; Chan, K. C.; Crooks, R. M. *J. Am. Chem. Soc.* **1997**, *119*, 189.

(9) Mowery, M. D.; Evans, C. E. Unpublished results.

(10) Schott, M. W.; Wegner, G. In *Nonlinear Optical Properties of Organic Molecules and Crystals*; Chemla, J., Ed.; Academic Press: Orlando, 1987.

(11) Lando, J. B. In *Polydiacetylenes*; Bloor, D., Chance, R., Eds.; Nijhoff: Dordrecht, The Netherlands, 1985.

(12) Wegner, G. *Z. Naturforsch.* **1969**, *24B*, 824.

(13) Tieke, B. In *Polymerization in Organized Media*; Paleos, C. M., Ed.; Gordon and Breach Science Publishers: Philadelphia, PA, 1992 and references therein.

(14) Okada, S.; Matsuda, H.; Nakanishi, H.; Kato, M.; Otsuka, M. *Thin Solid Films* **1989**, *179*, 423.

(15) Charych, D.; Nagy, J. O.; Spevak, W.; Bednarski, M. D. *Science* **1993**, *261*, 585.

(16) Reichert, A.; Nagy, J. O.; Spevak, W.; Charych, D. *J. Am. Chem. Soc.* **1995**, *117*, 829.

(17) Berman, A.; Ahn, D. J.; Lio, A.; Salmeron, M.; Reichert, A.; Charych, D. H. *Science* **1995**, *269*, 515.

(18) Kim, T.; Crooks, R. M.; Tsen, M.; Sun, L. *J. Am. Chem. Soc.* **1995**, *117*, 3963.

(19) Kim, T.; Ye, Q.; Sun, L.; Chan, K. C.; Crooks, R. M. *Langmuir* **1996**, *12*, 6065.

(20) Lin-Vien, D.; Colthup, N. B.; Fateley, W. G.; Grasselli, J. G. In *The Handbook of Infrared and Raman Characteristic Frequencies of Organic Molecules*; Academic Press: San Diego, CA, 1991.

(21) Evans, S. D.; Urankar, E.; Ulman, A.; Ferris, N. *J. Am. Chem. Soc.* **1991**, *113*, 4121.

(22) Amatore, C.; Saveant, J.-M.; Tessier, D. *J. Electroanal. Chem.* **1983**, *147*, 39.

(23) Chailapakul, O.; Crooks, R. M. *Langmuir* **1993**, *9*, 884.

(24) Creager, S. E.; Hockett, L. A.; Rowe, G. K. *Langmuir* **1992**, *8*, 854.

(25) Salmeron, M.; Neubauer, G.; Folch, A.; Tomitori, M.; Ogletree, D. F.; Sautet, P. *Langmuir* **1993**, *9*, 3600.

(26) Berman, A.; Ahn, D. J.; Lio, A.; Salmeron, M.; Reichert, A.; Charych, D. *Science* **1995**, *269*, 515.

(27) Hoper, R.; Gesang, T.; Possart, W.; Hennemann, E.-D.; Boseck, S. *Ultramicroscopy* **1995**, *60*, 17.

(28) Wawkuschewski, A.; Cramer, K.; Cantow, H.-J.; Magonov, S. N. *Ultramicroscopy* **1995**, *58*, 185.

(29) Li, Y.; Huang, J.; McIver, R. T.; Hemminger, J. C. *J. Am. Chem. Soc.* **1992**, *114*, 2428.

(30) Huang, J.; Hemminger, J. C. *J. Am. Chem. Soc.* **1993**, *115*, 3342.

(31) Tarlov, M. J.; Newman, J. G. *Langmuir* **1992**, *8*, 1398.